FALSE ATTACK ANGLE CAUSED by NUMERICAL DIFFUSION in 2D POTENTIAL FLOW PROBLEMS

Diomar Cesar lobão, dclobao@metal.eeimvr.uff.br
Universidade Federal Fluminese - UFF

Abstract. *A finite difference method is presented to predict external low speed and inviscid flow. The present paper intent to discuss 2D potential flow theory in generalized coordinate system (body-fitted coordinates) applied to numerical flow situations where unsymmetrical solutions are obtained. The numerical finite difference adopted for the governing equation discretization is solved by SOR and AF method. The computational procedure and its boundary conditions are presented and its effects on the numerical diffusion creating a false attack angle are treated. The problem is solved and a secondary solution, a fix is designed to eliminate the false attack angle. The flow past around a circular cylinder problem and also flow past around an airfoil are validated.*

Keywords*: Finite difference, SOR, AF method, false attack angle, Potential flow*

1. INTRODUCTION

This paper is about potential and incompressible flow. In engineering there are many applications where potential flow theory can be used to predict the nature of flow problems such as flow in pipes, free surface flow, and low speed external flow around 2D geometries. There are several numerical techniques applied to predict potential flow behavior. Their use coupled with the discrete boundary conditions applied on the solid wall via finite difference method and how the metrics are calculated can originated enough numerical diffusion which creates unrealistic numerical solution. The amount of numerical diffusion can reach such level that create false attach angle in a totally symmetrical flow on symmetrical geometry. The tangent flow boundary condition involving low order approximation for the metrics reveals to be responsible for such diffusion since generates different values for the potential where should be equal, the difference even small is enough to be visual. Elsewhere as discussed in (Virag and Trincas, 1994) the so called “false diffusion” has been noticed to be present with body-fitted coordinates. The amount of numerical diffusion is strongly dependent on the mesh size and on the quality of the mesh. When the flow is aligned with the mesh, numerical diffusion is minimized. The cylinder and equally the airfoil are typical geometry where the flow alignment with the mesh is not quite possible.

This paper is divided in the following manner: The elliptic grid generation is established and the airfoil geometry is defined. The potential flow equation is derived in generalized curvilinear coordinate system. The finite difference discretization is applied and the numerical methods for its integration are presented. The boundary condition are established and discussed. A fix algorithm is designed, when low order derivatives need to be used, to remove the numerical diffusion and finally some numerical simulations are shown.

2. ELLIPITIC GRID GENERATION

Grid generation techniques are designed to distribute points throughout the domain of a physical region, as well as on its bounding surfaces when they are required. The line connection of the points forms the grid and subdivides the physical region into a filling set of discrete volume or area elements. Types of structured grids (Thompson, 1987) and unstructured grids (Weatherill, 1988) have been used successfully to solve a wide range of problems in computational field simulation.

The strategy currently employed is to apply a mathematical transformation at the physical domain coordinates to a generalized body-fitted coordinate system, as $(x, y) \rightarrow (\xi, \eta)$, this same transformation is also used to transform the potential flow governing equation. The physical domain and computational domain are related as shown in the figure below.

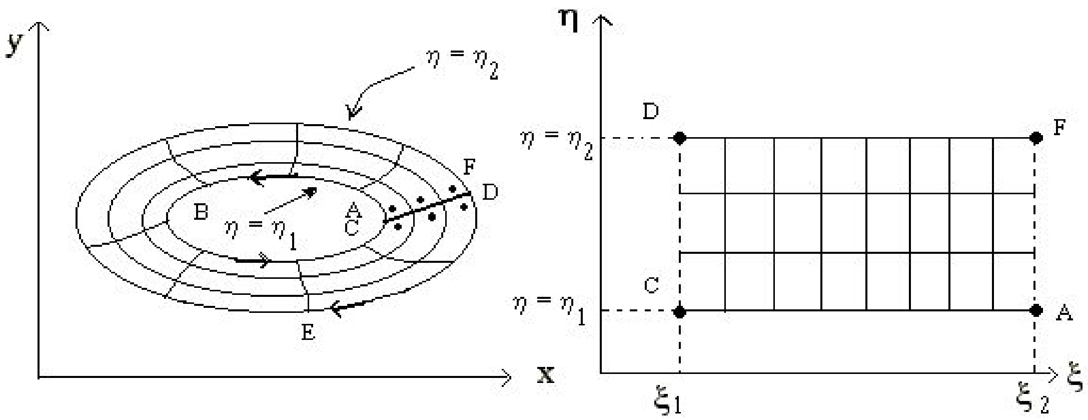

Figure 1. Double connected physical grid and the transformed computational domain.

The elliptic grid generation method is taken, that is, $\Delta\xi = \Delta\eta = 1$, and the governing equations for the grid coordinates nodes are:

$$\alpha x_{\xi\xi} + \gamma x_{\eta\eta} - 2\beta x_{\xi\eta} + \left(\frac{1}{J^2}\right)\left(Px_{\xi} + Qx_{\eta}\right) = 0 \tag{1}$$

$$\alpha y_{\xi\xi} + \gamma y_{\eta\eta} - 2\beta y_{\xi\eta} + \left(\frac{1}{J^2}\right)\left(Py_{\xi} + Qy_{\eta}\right) = 0 \tag{2}$$

Where

$$\alpha = g_{22} = x_{\eta}^2 + y_{\eta}^2,\ \gamma = g_{11} = x_{\xi}^2 + y_{\xi}^2,\ \beta = g_{12} = g_{21} = x_{\xi} x_n + y_{\xi} y_{\xi} \tag{3}$$

Are the metric tensor related to the transformation and *P* and *Q* are source functions used to concentrate lines where they are need, *P=Q=0* are used in the present situation. The iterative Gauss-Seidel method is applied to the eq (1) e eq (2) to get the final values of the coordinates $(x_{i,j}, y_{i,j})$ in the physical domain.

3. GOVERNING EQUATION

The mathematical and numerical formulation has been extensively documented (Anderson, 2001), (Robertson and Crowe, 1993). The governing equation written in the transformed curvilinear coordinate system (Subramanian and Chakrabartty, 1984), (Chipman, 1982) is given by

$$\frac{\partial^2\phi}{\partial\xi^2}\left(\xi_x^2 + \xi_y^2\right) + \frac{\partial^2\phi}{\partial\eta^2}\left(\eta_x^2 + \eta_y^2\right) + 2\frac{\partial^2\phi}{\partial\xi\partial\eta}\left(\xi_x\eta_x + \xi_y\eta_y\right) = 0 \tag{4}$$

where $\xi_x, \xi_y, \eta_x, \eta_y$ are the metrics of the transformation and are related to the physical domain by the following relations

$$\begin{matrix} \xi_x = Jy_{\eta} & \eta_x = -Jy_{\xi} \\ \xi_y = -Jx_{\eta} & \eta_y = Jx_{\xi} \end{matrix} \tag{5}$$

and the Jacobian is given by $J = \{x_\xi y_\eta - x_\eta y_\xi\}^{-1}$.

4. DISCRETIZATION AND NUMERICAL METHOD

Two numerical methods are used in order to solve the eq (4). The first one is the explicit Successive Over Relaxation SOR (White, 1994), (Chow, 1979). The second one is the Approximate Factorization method as an implicit unconditionally stable numerical method. The SOR method adopted makes use of the Gauss-Seidel method written as

$$\phi_{i,j}^{n+1} = \omega \Phi_{i,j}^{n+1} + (1-\omega)\phi_{i,j}^{n} \tag{6}$$

Where ω is the relaxation factor. Defining *RHS* as

$$\left(1 - \frac{\Delta t}{2} A \Delta_\xi^2\right)\left(1 - \frac{\Delta t}{2} B \Delta_\xi^2\right)\phi_{i,j}^{n+1} = RHS \tag{7}$$

Calling $\left(1 - \frac{\Delta t}{2} A \Delta_\eta^2\right)\phi_{i,j}^{n+1} = \phi_{i,j}^{*}$, then it is possible to write the two steps of AF method as follow:

- **1º step**: $\left(1 - \frac{\Delta t}{2} A \Delta_\xi^2\right)\phi_{i,j}^{*} = RHS$
- **2º step**: $\left(1 - \frac{\Delta t}{2} B \Delta_\eta^2\right)\phi_{i,j}^{n+1} = \phi_{i,j}^{*}$

(8)

In both numerical methods the term $2C\frac{\partial^2 \phi}{\partial \xi \partial \eta}$ has being studied. Its value is much small as compared to the main second order derivatives, although it is included, if removed will not bring any problem towards the steady state solution and does not affect the numerical solution stability as well as the numerical diffusion.

5. BOUNDARY CONDITION

As the cylinder/airfoil is solid it is required that, at the surface, the flow be tangential (Anderson, 2001) (Chow, 1979). Thus it is convenient to formally define this boundary condition by:

$$\frac{v}{u} = \left.\frac{\partial\phi/\partial y}{\partial\phi/\partial x}\right|_{\substack{solid\\wall}} = \frac{dy}{dx} \tag{9}$$

From the coordinate transformation it is known that: $dy = y_\xi d\xi + y_\mu d\xi$ and $dx = x_\xi d\xi + x_\eta d\xi$, however $d\eta = 0$ on the solid wall, since that the η line is bounded on the solid surface. Then it is possible to write the following relation

$$\frac{v}{u} = \frac{y_\xi}{x_\xi}, \text{implying } uy_\xi - vx_\xi = 0 \quad (10)$$

This tells that the *V contravariant* velocity must be zero, as

$$V = u\eta_x + v\eta_y = 0 \quad (11)$$

Making use of $\begin{cases} u = \xi_x \dfrac{\partial \phi}{\partial \xi} + \eta_x \dfrac{\partial \phi}{\partial \eta} + \overline{V}_\infty \\ v = \xi_y \dfrac{\partial \phi}{\partial \xi} + \eta_y \dfrac{\partial \phi}{\partial \eta} \end{cases}$ (12)

Using eq(12) substituting into eq(11) is possible to obtain the final boundary condition written as:

$$\frac{\partial \phi}{\partial \eta} = -\left[\frac{\partial \phi}{\partial \xi}\left(\xi_x\eta_x + \xi_y\eta_y\right) + \eta_x\overline{V}_\infty\right]\frac{1}{(\eta_x^2 + \eta_y^2)} \quad (13)$$

Added to this boundary condition is also need to enforce the periodical boundary condition at the wake line as shown in the fig. 1, by the lines AF and CD.

Kutta's condition provides a useful tool for the finite thickness airfoil (Anderson, 2001). This condition states that is required the flow to smoothly come off the trailing edge of the airfoil. However, this causes over determination of boundary condition, since the flow tangency is also applied there. Therefore, it is chosen to ignore the flow tangency condition at the trailing edge. Recent work (Anderson, 2001) specifies that unless the airfoil has a cusped trailing edge from which the flow may proceed smoothly, the velocity must go to zero at the trailing edge. This is implemented as:

$$\begin{cases} u = 0 \\ v = 0 \end{cases} \Rightarrow \begin{cases} \phi_{1,1} = \phi_{2,1} \\ \phi_{1,1} = \phi_{1,2} \end{cases} \quad (14)$$

6. FIX ALGORITHM FOR NUMERICAL DIFFUSION

The basic idea is simple enough to grasp. The correct application of the boundary condition given by eq(13) when the metrics are approximated by first order finite differences reveals to interactively generate enough numerical diffusion in order to create a false rotation in the flow field even when the sweep direction is changed around. This false rotation makes the flow field which is symmetrical on a symmetrical body looks as it has an attack angle, a "bogus" attack angle. The detailed observation, of the potential $\phi_{i,1}$ on the solid wall, reveals to be different on the upper and lower surfaces in opposite nodes. The following algorithm is designed to fix this when the first order finite difference is used to approximate the metrics and it is able to remove the overall numerical diffusion.

```
 for(i=1:nx-1)
   BC1(i,1) = eq(28)
end
for(i=nx-1:-1:1)
   BC2(i,1) = eq(28)
end
```

```
for(i=2:nx-1)
  if(BC1(i,1) == BC2(nx-(i-1),1))
      phi(i,1)=BC1(i,1);
  else
      phi(i,1)=(BC1(i,1)+BC2(nx-(i-1),1))/2.;
      phi(nx-(i-1),1)=phi(i,1);
  end
end
```

The two sweeps, one forward and the other backwards return unsymmetrical values. The upper values are tested with the lower surface values and if they are different they are changed by the average between the upper and lower values. If not the upper value is kept. The algorithm above achieves excellent results eliminating the numerical diffusion as well as the convergence rate is improved as will be shown in the next section.

7. RESULTS AND DISCUSSION

The following results are presented in an attempt to show that the numerical diffusion creates artifacts which are unrealistic solution. The SOR as well as AF method are equally affected by this unwanted effect. All numerical simulated solutions presented in this section are using a freestream velocity start of one. The simulations for the cylinder are carried out by the SOR method as for the airfoil is done by the AF method. The implicit method has two advantages, be stable and converge faster than the SOR as can be seen in residual history figures. Figure 2 shows the solution for the cylinder using first order finite difference approximation for the metrics.

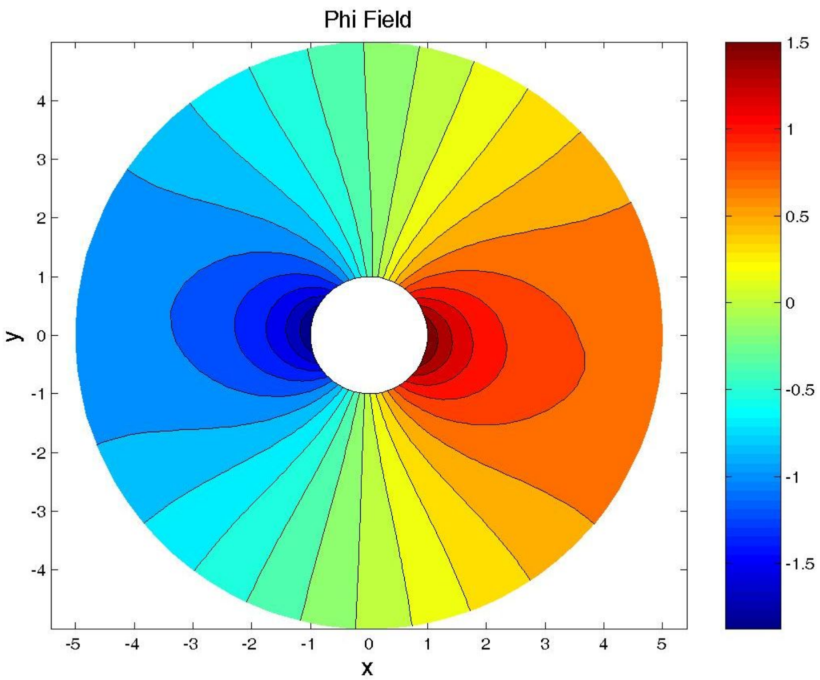

Figure 2. The potential flow field showing the false attach angle

As can be seen there is a false attack angle which is not expected. In the fig. 3 is shown the residual history calculated as norm L2. Is shown in the figure 4 a zoom where is easily visible the false attack angle generated by the numerical solution.

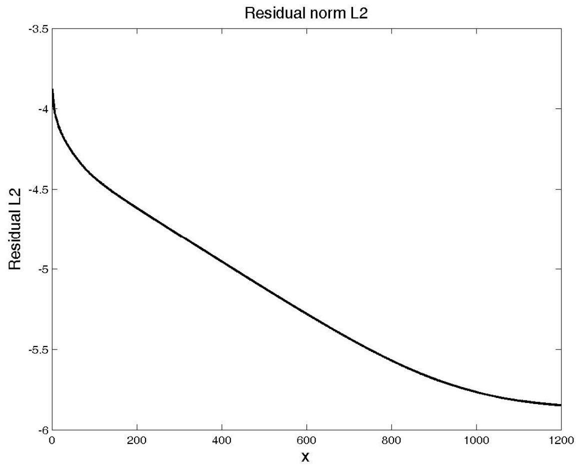

Figure 3. Residual history cylinder geometry

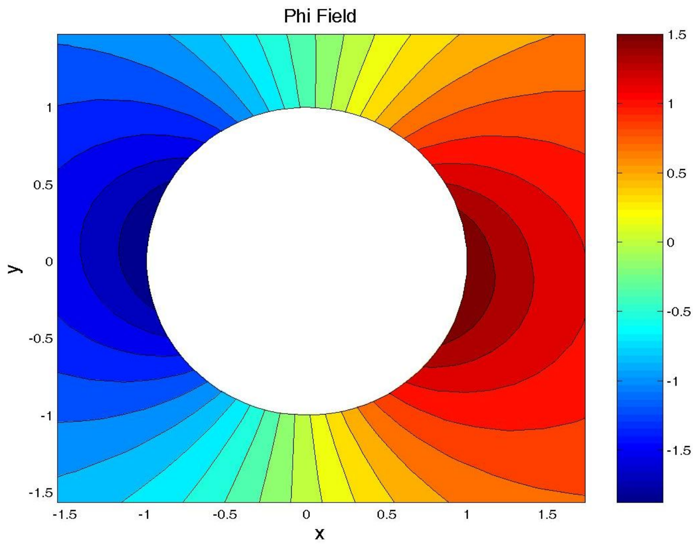

Figure 4. Zoom showing asymmetrical solution

In figure 5 is shown the result for the cylinder geometry making usage of the fix algorithm to recover the symmetry of the solution.

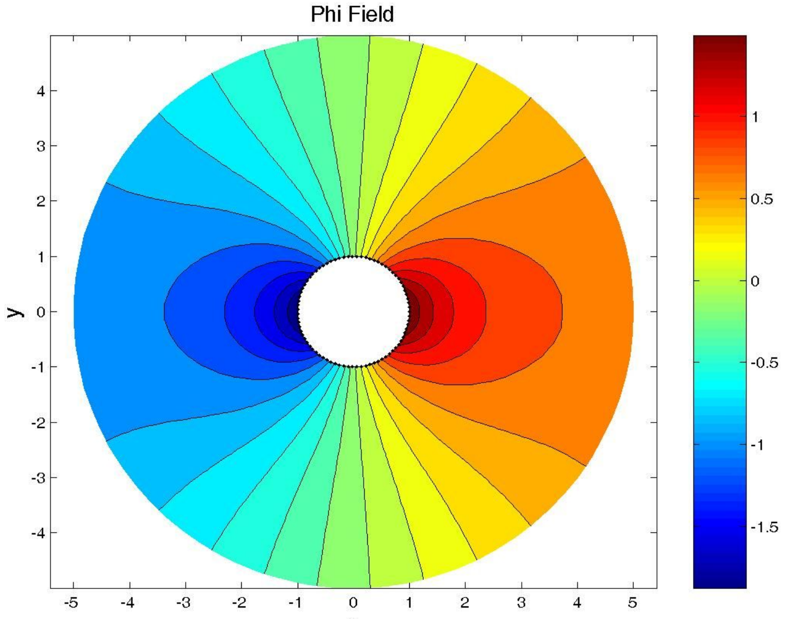

Figure 5. Solution for first order approximation for metrics plus fix algorithm

As can be seen the flow is symmetrical showing that the fix algorithm has recovered the expected solution. The figure 6 shows a zoom detail revealing the symmetrical field.

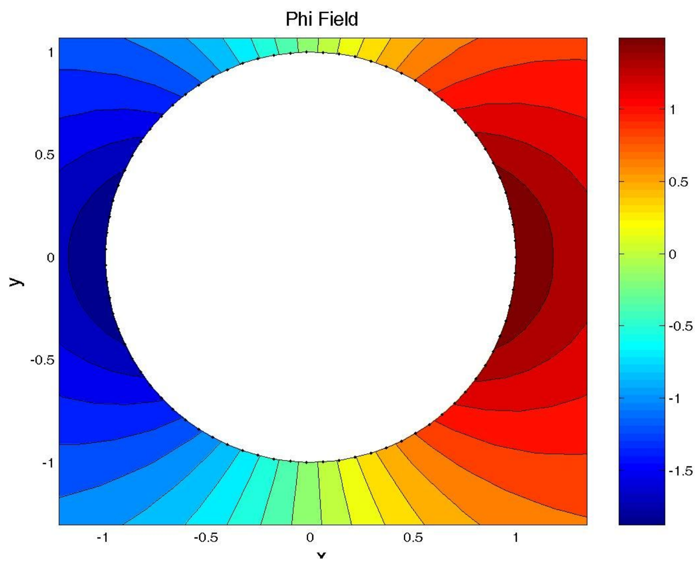

Figure 6. Zoom showing symmetrical solution

The figure 7 show the velocity flow field for the potential seen in the figure 6, its symmetry is easily noticed.

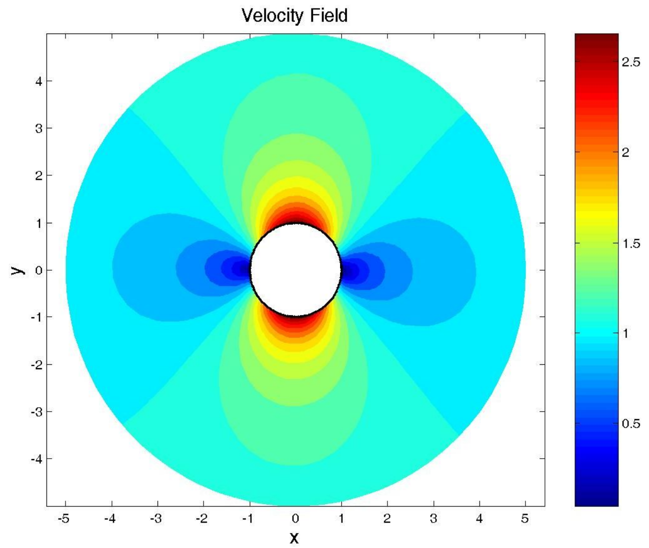

Figure 7. Velocity field

The next results are for the NACA0012 airfoil geometry. In the figure 8 is shown the potential function and as can be seen there is a false attack angle or unsymmetrical field.

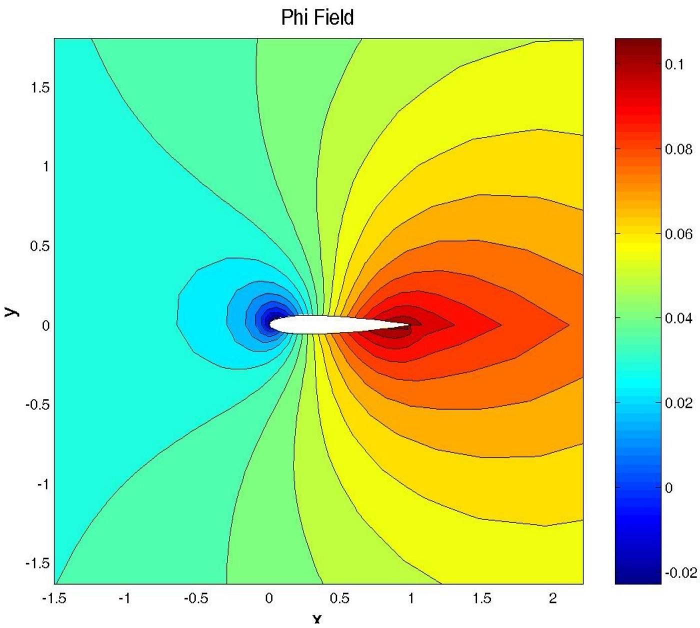

Figure 8. The potential for the airfoil NACA0012

The residual history for this simulation is shown in the figure 9.

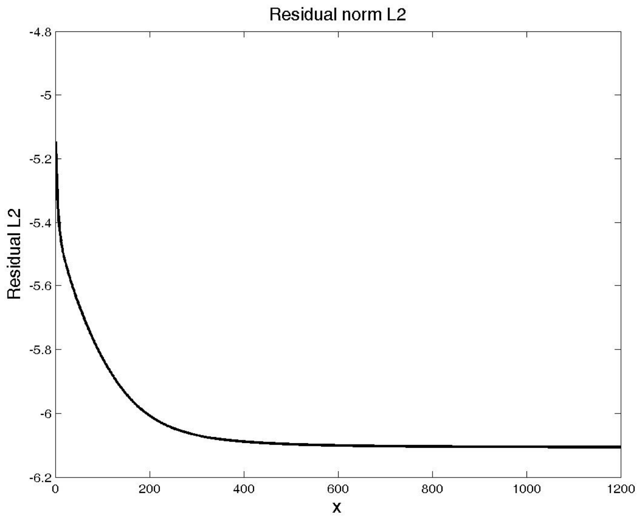

The figure 10 shows the simulation for the airfoil using the fix algorithm where the symmetrical solution is recovered.

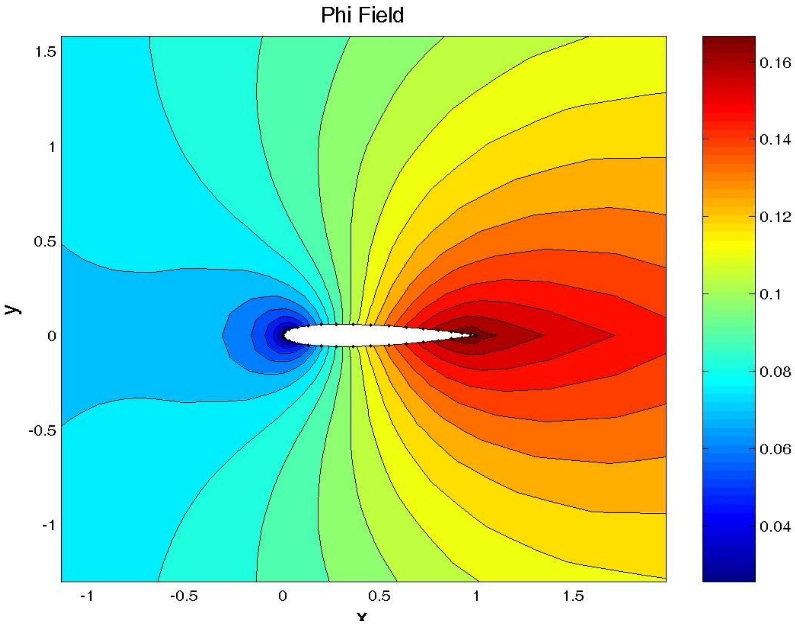

Figure 10. Zoom showing symmetric solution

In light of these results, it is clear that the fix algorithm proposed can be used to remove the numerical diffusion without compromise the solution convergence even when the first order finite difference is adopted. This fix algorithm doesn't need be used if since the beginning the second order finite difference approximation is adopted to the metric calculation.

8. CONCLUSION

This paper presents a finite difference method to solve 2D potential flow problems in generalized coordinate system. The mesh generation and numerical methods in its discretized form are shown. The proposed fix algorithm to recover the symmetry in the flow field is validated with two examples; a 2D cylinder with periodic boundary condition in the wake line, flow past an airfoil is also considerate. This algorithm is designed to correct symmetrical geometry flow and zero attack angle. The accuracy is compared against the fix algorithm. The results of the two examples show that the accuracy of the solution at the steady state using the fix algorithm. The "bogus" attack angle is generated by the pour approximation by finite difference for the metrics of the transformation, the second order approximation eliminates such numerical diffusion problem.

9. ACKNOWLEDGEMENT

The author is pleased to acknowledge Universidade Federal Fluminse and the Pensa Rio Project for supporting this research work.

10. REFERENCES

Thompson, J.F., 1987, "A General Three-Dimensional Elliptic Grid Generation System on a Composite Block Structure," *Comp. Meth. App. Mech. Eng.*, Vol. 64, pp. 377-411.

Weatherill, N.P., 1988, "A Method for Generating Irregular Computational Grids in Multiply Connected Planar Domains," *Int. J. Num. Methods Fluids*, Vol. 8, pp. 181-197.

Anderson, J.D., 2001, *Fundamentals of Aerodynamics*. 3rd Edition. Published by McGraw Hill Publishing.

Robertson, J.A. and Crowe, C.T., 1993, *Engineering Fluid Mechanics*, 5th edition, Houghton Mifflin, Boston, MA.

White, F.M., 1994, *Fluid Mechanics*, 3rd edition, McGraw-Hill, Inc., New York, N.Y.

Chow, C.Y., 1979, *Introduction to Computational Fluid Mechanics*. Published by John Wiley and Sons Publishing.

Subramanian, N.R. and Chakrabartty, S.K., 1984, "Computation of Inviscid Transonic Flow Past Aerofoils Using Body Fitted Coordinates", NAL Bangalore 560037.

Chipman, R. and Jameson, A., 1982, "Alternating-Direction Implicit Algorithm for Unsteady Potential Flow". AIAA Journal, vol. 20, issue 1, pp. 18-24.

Virag, Z., Trincas, G., 1994, "An improvement of the exponential differencing scheme for solving the convection-diffusion equation". Advances in Engineering Software. Vol. 19, pp 1-19.

11. RESPONSIBILITY NOTICE

The author is the only responsible for the printed material included in this paper.